AIAA 98-2694

A Novel Investigation of the Oscillatory Field Over a Transpiring Surface

J. Barron and W. K. Van Moorhem
University of Utah
Salt Lake City, UT 84112

J. Majdalani
Marquette University
Milwaukee, WI 53233

2nd AIAA Theoretical Fluid Mechanics Meeting
June 15–18, 1998
Albuquerque, NM

A Novel Investigation of the Oscillatory Field Over a Transpiring Surface

J. Barron* and W. K. Van Moorhem†
University of Utah, Salt Lake City, UT 84112
and
J. Majdalani‡
Marquette University, Milwaukee, WI 53233

The flowfield character is investigated inside a long rectangular chamber in the presence of time-harmonic pressure waves. The chamber is designed with multiple interchangeable sections for the purpose of controlling the length and therefore the system's natural frequency. Pressure waves are induced externally at variable frequencies by means of a Scotch-yoke mechanism capable of imparting pure oscillatory motions. In characterizing the internal flowfield, velocity measurements are acquired inside a principal test section that can accommodate flat blocks of solid carbon dioxide (a.k.a., dry ice). As solid CO_2 sublimates, a flow of gaseous carbon dioxide transpires from the bottom of the principal section and enters the chamber in the transverse direction. The resulting Stokes layer formed above the transpiring surface exhibits several features associated with oscillatory flows over impermeable surfaces, including an overshoot in the velocity amplitude in the vicinity of the transpiring wall known as Richardson's annular effect. Quantitative pressure and velocity measurements are in agreement with theoretical predictions obtained from recent models of the oscillatory field over transpiring surfaces. Since the sublimation rate of dry ice can be expressed in a similar mathematical form to the regression rate at the burning surface of solid propellants, this experiment constitutes a cold flow simulation of the internal flowfield in solid rocket motors.

I. Introduction

Going back through available literature, only few experimental investigations are found that address the nature of the oscillatory flowfield over a transpiring surface. This may be attributed to the inherent difficulty in designing and measuring flow parameters in such unsteady environments in the absence of analytical formulations to help in the planning process. Motivation, the mother of invention, arose, not long ago, from the need to understand and resolve the internal fluid dynamical coupling inside rocket chambers where the flow consists essentially of a coupling between gases injected inwardly and the oscillatory waves triggered by unsteady combustion.

In the hope of elucidating the nature of the resulting flowfield, an experimental investigation was conducted by Brown and co-workers[1-4] who used Nitrogen gas injection through uniformly sintered bronze plates in a cylindrical chamber of a circular cross section wherein acoustic waves were generated from an externally located rotating valve. Brown's results verified the accuracy of the analytical model suggested by Culick[5] for the mean flowfield and also provided substantial data for the resulting acoustic field. Independently of Brown's work, a novel experimental facility was built by Ma[6-9] to simulate similar flowfield conditions in a rectangular chamber. The variance in Ma's experiment was that it employed the sublimation of carbon dioxide, a process that resembles the propellant response to combustion, in generating the CO_2 gas at the transpiring wall.

Ma measured pressure, velocity, and mass flow rates of solid carbon dioxide as a function of frequency in his experiments. Unfortunately, the work by Ma had experimental difficulties in measuring acoustic pressure and velocity because he used a slider-crank mechanism consisting of a cylindrical piston, connecting rod, and crankshaft arrangement as the wave generator. Since the wave motion produced by a slider-crank mechanism is not purely sinusoidal, Ma's wave generator produced

*Currently Head of Mechanical Engineering, Halff Associates, Inc., Dallas, TX 75225. Member AIAA.

†Professor, Department of Mechanical Engineering. Senior Member AIAA.

‡Assistant Professor, Department of Mechanical and Industrial Engineering. Member AIAA.

many harmonics that complicated the spectral analysis of acoustic data. Ma thought that turbulence occurred in his experiments. However, due to the complex acoustic waves and lack of statistical data, Ma's experiments did not have the capability to verify the occurrence of turbulence.

In the current work, the problem encountered in Ma's investigation will be remedied first by eliminating the sources of harmonics and second, by employing a reliable statistical data acquisition package. The first improvement is achieved by utilizing a Scotch-yoke mechanism to replace the slider-crank mechanism that was used previously.

Another purpose of this investigation is to compare experimental data to predictions derived from analytical models of the flowfield by Flandro[10] and Majdalani.[11]

To summarize, the purpose of this paper will be to discuss the design and present the results of an experimental investigation of the oscillatory velocity field over a transpiring surface that can validate recent theoretical formulations. The advantages of using the current experimental setup to obtain reliable data will be stated along with a brief review of previously used approaches. The principal advantage of the current setup is that it employs a Scotch-yoke mechanism to produce a purely harmonic motion, thus eliminating undesired secondary frequencies arising from the use of other driving mechanisms. The transpiring surface consists of sublimating dry ice and the working fluid is carbon dioxide. Experimental data sets will be compared and shown to be agreeable with recent analytical and numerical solutions for the velocity flowfield established in such an environment.

II. Improved Wave Generator

Different mechanisms are used to produce the oscillatory motion: slider-crank, rotating valves, scotch-yoke, etc. Schematics of such devices are furnished below (see Fig. 1). Electrical motors or small internal combustion engines are popular examples of drivers used to produce the desired oscillatory motion.

The piston position for a crankshaft-connecting rod system is given by the expression:

$$x = r\cos(\omega t) + l\sqrt{1-\left(\frac{r}{l}\right)^2 \sin^2(\omega t)} \qquad (1)$$

where r is the offset of the crankshaft throw and l is the length of the connecting rod (r/l about 1/4 generally). When this motion is expressed in the form of Fourier series with the assumption of small values of r/l, the series that ensues is:

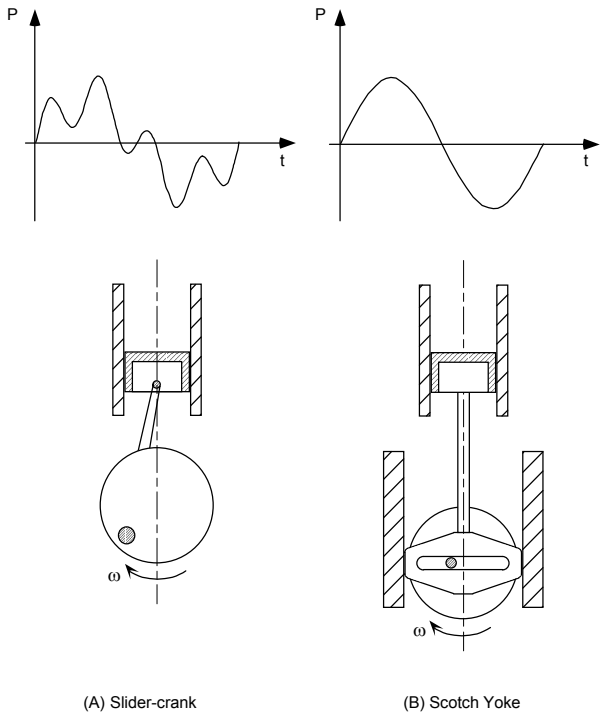

Fig. 1 Pressure vs. time for (A) piston with slider-crank configuration, and (B) piston with scotch yoke configuration.

$$x = l\left(1-\frac{1}{4}z^2-\frac{3}{64}z^4+\ldots\right)+r\cos(\omega t) + l\left(\frac{1}{4}z^2-\frac{1}{16}z^4+\ldots\right)\cos(2\omega t) + l\left(-\frac{1}{64}z^4+\ldots\right)\cos(4\omega t)+\ldots \qquad (2)$$

where $z = r/l$. In reality, terms with z to powers higher than four can be ignored for typical devices. This series clearly points out that only odd harmonics of the fundamental frequency should be seen. In actuality, all the harmonics are seen, not only the odd harmonics. This is due to nonideal piston motion caused by the looseness in the bearings.[7] If all the harmonics are present, then a solution for the gas velocity u' in a tube is likely of the form:

$$u' = \frac{u_1}{\sin(kl)}\sin\left[k(L-x)\right]\cos(\omega t) + \frac{u_2}{\sin(2kl)}z\sin\left[2k(L-x)\right]\cos(2\omega t) + \frac{u_3}{\sin(3kl)}z^2\sin\left[3k(L-x)\right]\cos(3\omega t)+O(z^3) \qquad (3)$$

where u_1, u_2, and u_3 are constants.[7]

Resonance will hence occur when the piston frequency is $1/m$ of the fundamental natural frequency, since now $\sin(mkl) = 0$ at resonance:

$$f_0 = a_0/(2L);\ f_m = a_0/(2mL);\ \ m = 1, 2, \ldots \qquad (4)$$

In these higher fractional cases, since the driving amplitude is smaller than the fundamental one, a much weaker excitation is observed. Theoretically, resonance should also occur when the piston is running at one fourth (or even smaller fractions) of the natural frequency of the chamber: These resonant peaks are usually negligible due to the weak driving amplitude of the order of z to the third or higher power. Thus for realistic values of z, one would expect large amplitudes around $f = a_0/(4L)$, $a_0/(3L)$, $a_0/(2L)$, and a_0/L, etc.

As shown in Fig. 1, the slider-crank mechanism does not produce a pure sinusoidal piston motion. Since the piston movement is not purely sinusoidal, many harmonics are introduced into the acoustic velocity and pressure fields. The sketch of pressure vs. time demonstrates the harmonics that complicate the acoustic data when using the slider-crank arrangement. The added harmonics in the acoustic data make it very difficult to do meaningful statistical and Fourier analyses for determining the occurrence of turbulence. The scotch yoke, as shown by a plot of pressure vs. time in Fig. 1, provides a pure sinusoidal piston motion, leading to improved control over the fundamental frequency and harmonics of the oscillating pressure and velocity fields.

III. Experimental Facility

A. Description

The Solid Carbon Dioxide Simulation Facility is a "cold flow" (nonreactive) facility (Fig. 2). The use of solid carbon dioxide (dry ice) is to simulate the internal flowfield of a solid propellant rocket motor. The use of dry ice as the simulated propellant makes it possible to focus on the fluid mechanics of the acoustic instability problem by separating the fluid mechanics from combustion of actual propellant. The flow chamber has a square cross section with an inside dimension of 7.62 by 7.62 centimeters. The flow chamber consists of eight interchangeable sections, a test section used for flow measurement, and a vibration isolating tube. The entire flow chamber is bolted to a heavy granite table to minimize vibration. The interchangeable sections make it possible to vary the test section location, chamber length and system resonant frequency. For these experiments, the length was held constant at 2.83 meters corresponding to a resonant frequency of 49 Hz at a temperature of 27 °C.

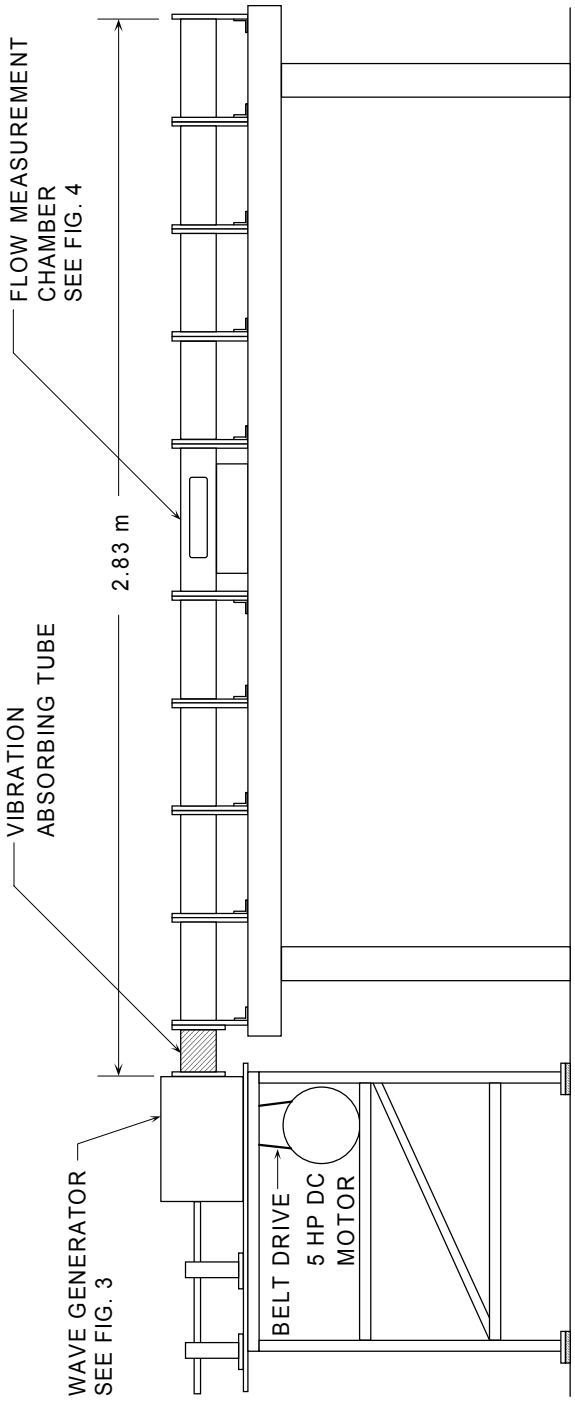

Fig. 2 Experimental apparatus.

B. Experimental Configurations

Two types of experiments were performed. The first set of experiments were done without dry ice in the flow chamber at driving frequencies ranging between 2.3 and 44.8 Hz. The second set of experiments were carried out with dry ice in the flow chamber to simulate

burning propellant at driving frequencies ranging between 2.2 and 50.8 Hz. For all experiments, the chamber was initially purged with room temperature CO_2 gas to remove the air. The CO_2 gas enters at one end of the flow chamber and exits the chamber at the opposite end through a small orifice which is closed with a valve prior to operating the wave generator.

C. Wave Generator

A wave generator located at one end of the flow chamber was used to produce an acoustic environment inside the chamber. A mechanical driving system based on a Scotch-yoke mechanism was designed and built (see Fig. 3). The wave generator has a volumetric displacement of 232 cm^3 and is driven by a 3.7 kilowatt variable speed DC motor. The connecting rod has a linear motion and is supported by two linear bearings. The connecting rod is connected rigidly to the piston and the Scotch-yoke. The scotch yoke also has a linear motion and has a slot for crankshaft travel, theoretically resulting in a pure sinusoidal piston motion. The flow chamber is isolated from vibration caused by the wave generator and motor by a vibration isolating tube between the wave generator and the flow chamber and neoprene pads under the feet of the flow chamber support structure.

D. Principal Test Section

The center section of the flow chamber is a 43.2 cm long test section (see Fig. 2). The test section was placed near the center of the chamber where the acoustic velocity antinode (maximum velocity) occurs and a pressure node (pressure minimum) occurs for a standing wave. This setup minimizes any pressure type of coupling in the dry ice sublimation. Figure 4 shows a section view of the test section. Solid carbon dioxide (dry ice) is used in the test section to simulate solid propellant rocket motor characteristics. The sublimation of the solid CO_2 into gaseous carbon dioxide simulates the burning of the propellant. The solid CO_2 is a commercial dry ice block approximately 30 cm long, 5 cm deep, and 7.62 cm in width which is equal to the width of the test section. The dry ice rests on a wooden block and a bellows is used to maintain the top of the dry ice at the same level as the bottom of the test section. The bellows pushes the dry ice with a constant supply air pressure of 3 psig. The bellows supply pressure is sufficiently large to eliminate significant vibration of the dry ice block due to acoustic pressure oscillations on the top dry ice surface. The dry ice can be replaced with a fitted aluminum plate that makes the investigation of the flowfield without side-wall injection possible. Glass view ports are located on either side of the test section to facilitate visual flow monitoring. The velocity of the gas near the surface of the dry ice can be measured by hot film anemometry.

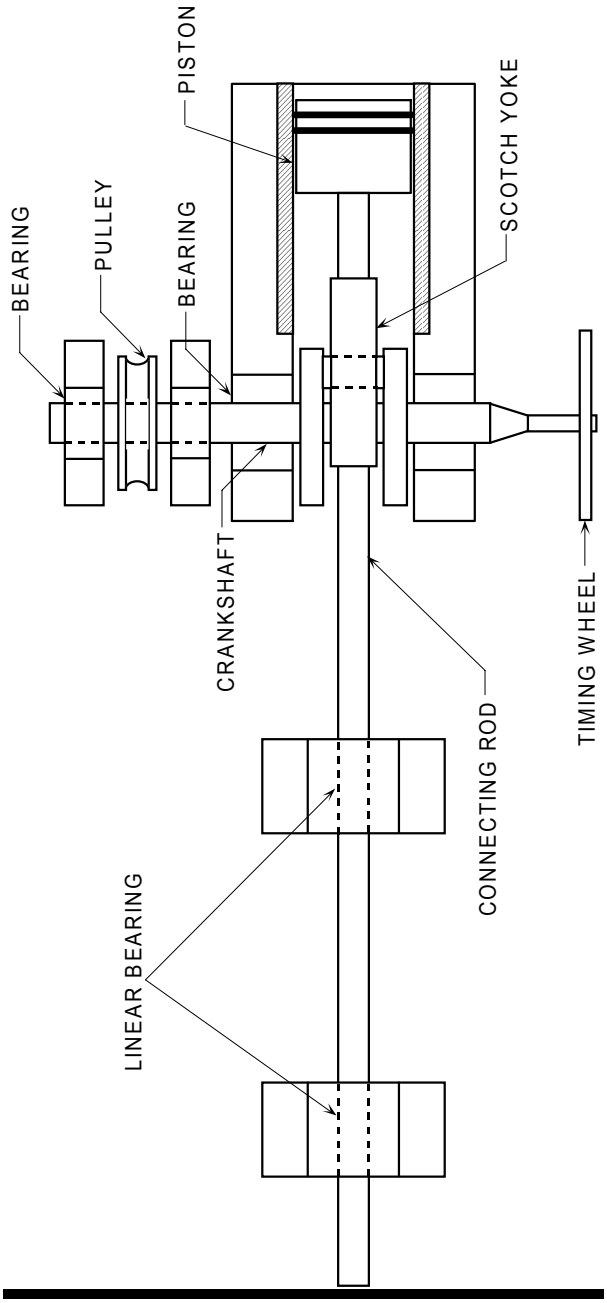

Fig. 3 Wave generator.

E. Hot Film Anemometry

A hot film anemometer is mounted in the test section as shown by section A-A in Fig. 5. The hot film probe is centered above the dry ice and is located approximately 0.8 cm above the surface of the dry ice. The hot film probe is mounted perpendicularly to the dry ice surface.

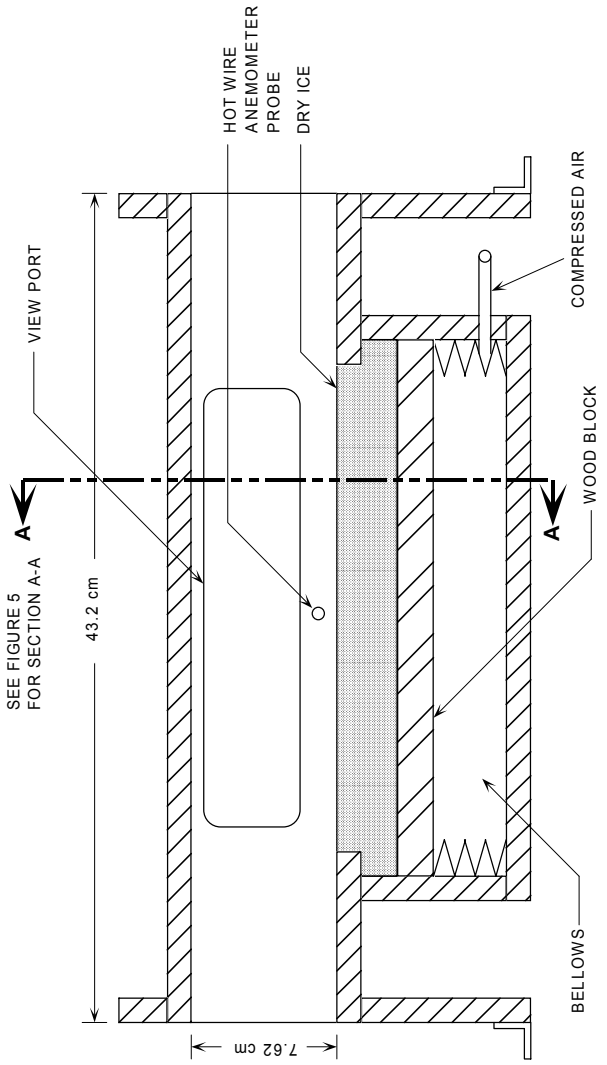

Fig. 4 Flow measurement chamber.

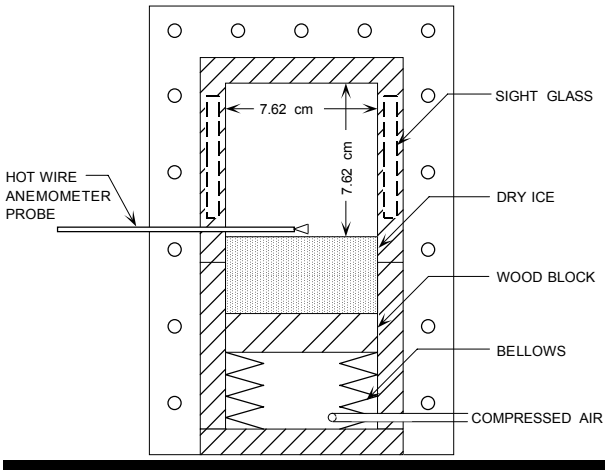

Fig. 5 Section A-A: Flow measurement section.

F. Pressure Measurement

Pressure oscillations in the flow chamber can also be measured. A pressure transducer can be mounted at various locations in the chamber to record the pressure oscillations. For these experiments the pressure transducer was located at the end of the flow chamber opposing the wave generator where maximum pressure is observed.

The volumetric displacement of the wave generator is 262 cm^3, resulting in a larger pressure amplitude than in previous research. Increasing the pressure over the solid CO_2 results in an increase in the sublimation rate and mass flow from the surface due to the decrease in the heat of sublimation with increasing pressure. Ma[7] used an infrared light above the dry ice to increase the sublimation rate. The infrared light also heated the hot film probe, resulting in zero bridge voltage and electronic oscillations in the anemometer control circuit which made velocity measurements impossible. By increasing the oscillating pressure amplitude instead of using an infrared heat lamp, velocity measurements with the hot film probe were facilitated.

IV. Instrumentation

The instrumentation used to acquire velocity and pressure data from the Solid Carbon Dioxide Simulation Facility is described in this section and is shown schematically in Fig. 6. An acoustic flowfield is produced in the flow chamber by a wave generator. The wave generator is powered by a 3.7 kilowatt DC motor and power supply. The driving frequency of the piston is controlled by a potentiometer connected to the power supply. A highly sensitive pressure transducer (Kistler model 606L) is used for monitoring pressure oscillations generated in the flow chamber. A charge amplifier (PCB model 464A) converts voltage signals from the piezoelectric pressure transducer to

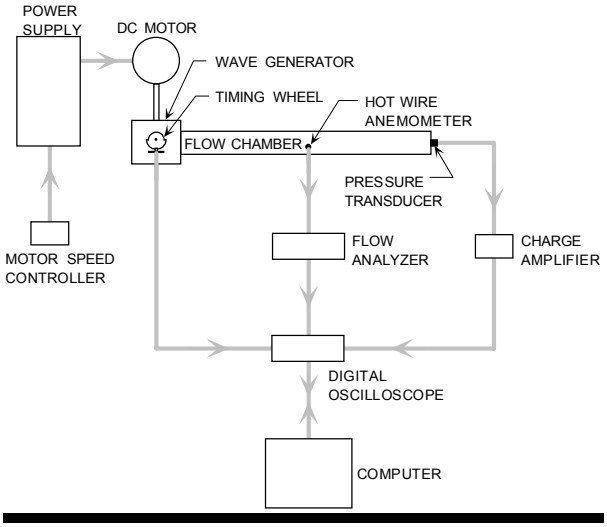

Fig. 6 Experimental system.

standardized voltage signals compatible with readout instruments. The resultant voltage signal then goes to a digital oscilloscope (HP model 54501A) where the pressure data is digitized. The computer gets the pressure data from the oscilloscope and saves the data for analysis. A low noise, constant temperature hot film probe (TSI model 1210-60) is used to measure velocity oscillations generated in the flow chamber. The flow analyzer (Intelligent Flow Analyzer model 100) converts the current from the sensor to a voltage proportional to velocity. The flow signal conditioner also filters unwanted noise and amplifies the signal. The analog velocity signal goes from the flow analyzer to the oscilloscope where it is digitized. The computer gets the velocity data from the oscilloscope and stores the data for analysis.

V. Operation

In order to perform statistical analyses, multiple acoustic velocity and pressure data sets at a given frequency needed to be collected with the same starting point in the mechanical driving cycle. A timing wheel and a timing signal were implemented to consistently begin the collection of each data set at the same point in the mechanical driving cycle (see Fig. 7). The timing wheel was mounted on the crankshaft as shown by Fig. 3. The outer portion of the timing wheel is centered in a slot which has a light sensor that is blocked when the large radius portion of the timing wheel rotates through the slot as shown in Fig. 7. When the timing wheel rotates so that the large radius portion of the timing wheel is not in the slot, the light is not blocked and the timing circuit is closed. The resulting timing signal is a square wave. Data are collected when the computer sends a signal to the oscilloscope to start collecting data and the timing wheel rotates to the point where the timing circuit is closed. Acoustic data (either velocity or pressure) is then collected at the oscilloscope and sent to the computer to be stored. The pressure and velocity data acquired in the experiments was Fourier analyzed to demonstrate the reliability of the driving mechanism.

In order to do a statistical analysis of the data, between 10 and 15 data sets were collected at a given piston driving frequency. The data sampling frequency was varied with frequency of the driving piston. Each data set consisted of 512 data points which were collected during a time period of approximately two driving piston cycles. Since the piston frequency was varied between 2.2 and 50.8 Hz, the sampling frequency varied between 512 and 10,240 Hz.

Calibration of the hot film anemometer is extremely important. The sensing elements are delicate mechanically and analog output signals have a tendency to drift so frequent checks of probe calibration are necessary. Hot film anemometers are very repeatable so accuracy is a function of how closely the calibration conditions are being reproduced in the flow to be measured. Calibration was performed before each data set was acquired. A flow generator with a plenum chamber and an ASME nozzle were used to get a known air velocity for calibration. The nozzle exit velocity was determined from Bernoulli's equation. An assumption that the static pressure of the air exiting the nozzle is equal to the outside atmospheric pressure was used. A calibration relationship was determined between known velocity and bridge voltage with the hot film probe located at the nozzle exit. The relationship is nonlinear (approximately a ¼ power relation). Figure 8 shows a typical hot film calibration curve. In Fig. 8, the horizontal axis is the known air velocity from the ASME nozzle. The vertical axis represents the voltage output from the hot film anemometer.

VI. On the Stokes Layer

Due to the prevalent oscillatory motion, the boundary layer formed over the surface is of the Stokes type. Let us recall that the Stokes layer over a hard wall is a region where viscous and rotational flow conditions persist in an oscillatory fluid due to the presence of solid boundaries.[12] The thickness of this region is

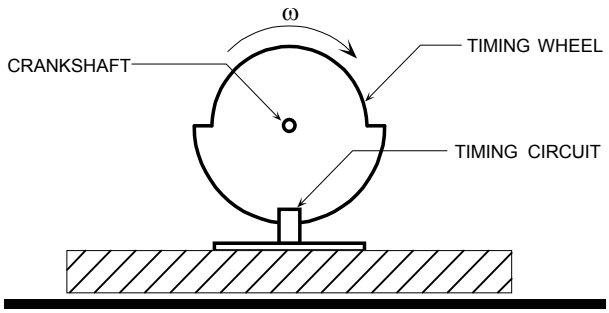

Fig. 7 Timing wheel.

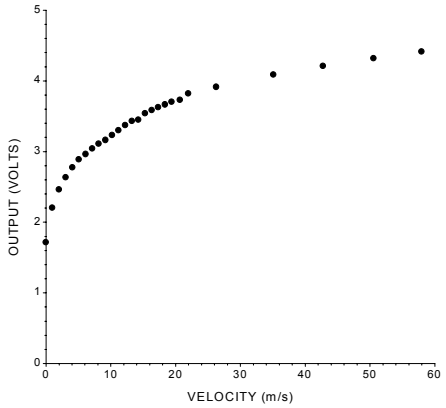

Fig. 8 Calibration curve of a hot film anemometer.

determined by viscosity and frequency and does not grow with time or distance. The idea behind this characteristic length can be clarified by looking at the case known as Stokes' Second Problem.[12] In that problem, Stokes[13] considers an inertial, viscous, incompressible and two-dimensional fluid in contact with an infinitely long plate that is in oscillatory motion. The velocity field is readily found to be

$$u(y,t) = U_0 e^{-\sqrt{\frac{\omega}{2\nu}}y} \cos\left[\omega\left(t - \frac{y}{\sqrt{2\omega\nu}}\right)\right] \qquad (5)$$

which describes a decaying wave traveling in the $+y$ direction (away from the wall). The frequency of oscillations is given by: $f = \omega/(2\pi)$. The speed of wave propagation is $\sqrt{2\omega\nu}$, which indicates that larger frequency or kinematic viscosity lead to larger propagation rate of disturbances. At a sufficiently large distance from the solid boundary, the flow can be considered to be unaffected by the presence of the wall. Stokes[13] introduces a length scale $\delta_{st} = 2\sqrt{2\nu/\omega}$ such that when the distance from the wall is equal to δ_{st}, the amplitude of the velocity will have reached 13.5% of its initial value. Other researchers define the Stokes boundary layer thickness to be equal to one wavelength $\lambda_{st} = 2\pi\sqrt{2\nu/\omega}$ for which the velocity amplitude will have reached 0.2% of its initial value. Evidently, a layer that scales with $\sqrt{\nu/\omega}$ is indicative of the domain where the flow is affected by the presence of solid boundaries and local no-slip conditions. This scale is in many ways analogous to the boundary layer thickness encountered in nonperiodic flows.

VII. Comparison for a Hard Wall

For the case without dry ice, the experimentally measured amplitudes of acoustic oscillations recorded by the hot film match quite closely the theoretical values predicted from a one-dimensional, inviscid and irrotational acoustic solution in the chamber. This is to be expected since the flow can be considered to be inviscid everywhere except in the vicinity of the walls where a thin Stokes layer is formed. Hot film measurements confirm that, outside of the Stokes layer, the motion in the so-called "outer region" can be well modeled by an inviscid and irrotational acoustic theory. In most test cases conducted, the Stokes boundary layer was smaller than the vertical distance from the wall to the tip of the hot film. Viscous and rotational effects, including slight longitudinal velocity overshoot, were found to be insignificant outside the Stokes boundary layer.

VIII. Comparison for a Transpiring Wall

For the case with dry ice, when side-wall injection of CO_2 is present, the experimentally measured amplitudes of acoustic oscillations recorded by the hot film are about one and a half times larger than the theoretical values predicted from a one-dimensional, inviscid and irrotational acoustic solution. This is to be expected since, when side-wall injection is present, the resulting boundary layer near the dry ice surface is significantly larger than before (without injection). The location of the hot film happens to fall inside the boundary layer region which is highly rotational and viscous. As shown by several researchers, including Flandro,[10] and Majdalani,[11] a two-dimensional time-dependent field is more adequate to describe the flow velocity inside the laminar boundary layer. One important phenomenon exhibited by the velocity profile inside the boundary layer is the presence of a so-called Richardson[14] velocity overshoot near the wall of a magnitude almost twice the one-dimensional acoustic wave amplitude in the outer region. This overshoot is maximal near the wall and decays to one at the edge of the boundary layer with a spatial average of 1.5 within the boundary layer. When turbulence occurs, one would expect the boundary layer to be even larger due to enhanced randomness and three dimensionality. Since the hot film is located somewhere within the boundary layer, it is therefore expected for the measured wave amplitudes to be larger than the one-dimensional wave amplitudes by a factor ranging from 1 to 2. The experimental error associated with determining exactly what this overshoot factor is can be enormous due to the compounded uncertainties in measuring the injection speed of CO_2, the kinematic viscosity of the gas around the hot film, the location of the hot film, and the actual frequency of oscillations, all of which are needed to determine the exact amount of overshoot (refer to Majdalani's dissertation[11] for a detailed discussion of the overshoot phenomenon and its prediction). For turbulent flows in our experiment, since the experimentally measured amplitudes are about one and a half times larger than the one-dimensional wave amplitudes, it can be concluded that an agreement with the most current theories is in place (see Fig. 9).

When using the two-dimensional time-dependent solutions provided by Majdalani for a rectangular geometry,[11] an excellent agreement is found to exist between analytical predictions and experimental results. This eliminates the need to address the issue of whether or not velocity coupling or flow turning mechanisms are present since no further corrections are required to achieve an agreement between theory and experiment.

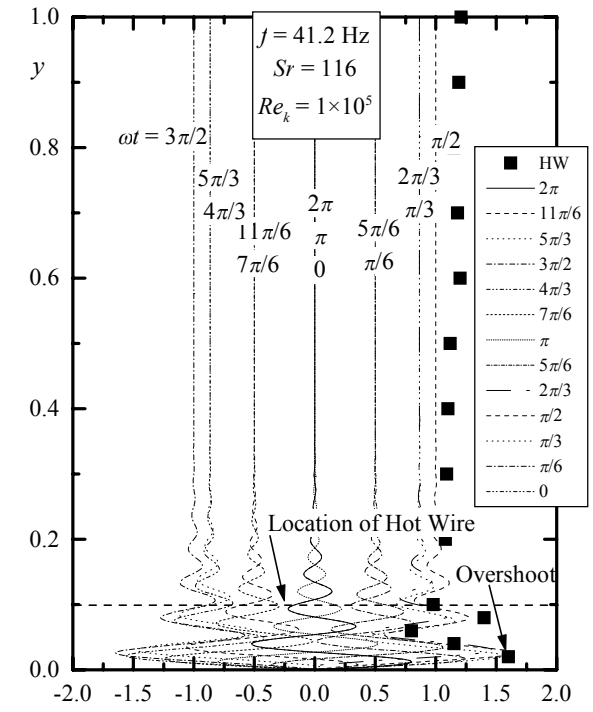

a)

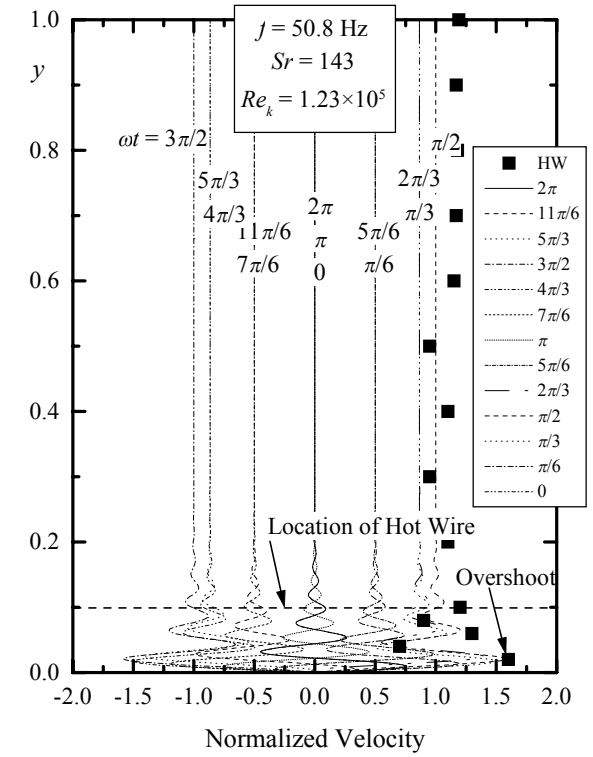

b)

Fig. 9 Timelines of the oscillatory velocity (normalized by the acoustic wave amplitude) near the dry-ice surface compared to recent theories for (a) f = 41.2 Hz and (b) f = 50.8 Hz.

IX. Conclusions

In this work, a novel experimental facility is built to investigate the characteristics of the oscillatory/acoustic flowfield over a transpiring surface. It is ascertained that the use of a Scotch-yoke mechanism is very well suited to produce purely harmonic motions. As a result, accurate velocity measurements are successfully acquired and correlated. The experimental data sets furnished are unbiased, being the result of a purely harmonic driver.

The results show a velocity overshoot near the wall that is characteristic of oscillatory flows in general (over permeable and impermeable walls). This so-called Richardson velocity overshoot occurs near the wall due to the phase difference between acoustic and vortical waves.

Comparisons to analytical and numerical predictions demonstrate a fair agreement with current theory. In a sense, this investigation provides an experimental verification for the analytical formulation of the oscillatory velocity field in a rectangular channel with mean transmission of a transverse flow.

References

[1]Brown, R. S., Erickson, J. E., and Babcock, W. R., "Measuring the Combustion Response of a Forced Oscillation Method," *AIAA Journal,* Vol. 12, No. 11, 1974, pp. 1502-1510.

[2]Brown, R. S., Blackner, A. M., Willoughby, P. G., and Dunlap, R., "Coupling Between Acoustic Velocity Oscillations and Solid Propellant Combustion," *Journal of Propulsion and Power,* Vol. 2, No. 5, 1986, pp. 428-437.

[3]Brown, R. S., Blackner, A. M., Willoughby, P. G., and Dunlap, R., "Coupling Between Velocity Oscillations and Solid Propellant Combustion," AIAA Paper 86-0531, Jan. 1986.

[4]Shaeffer, C. W., and Brown, R. S., "Oscillatory Internal Flow Studies," Chemical Systems Div. Rept. 2060 FR, United Technologies, San Jose, CA, Aug. 1992.

[5]Culick, F. E. C., "Rotational Axisymmetric Mean Flow and Damping of Acoustic Waves in a Solid Propellant Rocket," *AIAA Journal,* Vol. 4, No. 8, 1966, pp. 1462-1464.

[6]Ma, Y., Van Moorhem, W. K., and Shorthill, R. W., "Innovative Method of Investigating the Role of Turbulence in the Velocity Coupling Phenomenon," *Combustion Instabilities Driven by Thermo-Chemical Acoustic Sources*, NCA Vol. 4, HTD Vol. 128, American Society of Mechanical Engineers, New York, 1989, pp. 17-22.

[7]Ma, Y., "A Simulation of the Flow Near a Burning Propellant in a Solid Propellant Rocket Motor," Ph.D. Dissertation, University of Utah, 1990.

[8]Ma, Y., Van Moorhem, W. K., and Shorthill, R. W., "Innovative Method of Investigating the Role of Turbulence in the Velocity Coupling Phenomenon," *Journal of Vibration*

& Acoustics-Transactions of the ASME, Vol. 112, No. 4, 1990, pp. 550-555.

[9]Ma, Y., Van Moorhem, W. K., and Shorthill, R. W., "Experimental Investigation of Velocity Coupling in Combustion Instability," *Journal of Propulsion and Power,* Vol. 7, No. 5, 1991, pp. 692-699.

[10]Flandro, G. A., "Effects of Vorticity Transport on Axial Acoustic Waves in a Solid Propellant Rocket Chamber," *Combustion Instabilities Driven by Thermo-Chemical Acoustic Sources*, NCA Vol. 4, HTD Vol. 128, American Society of Mechanical Engineers, New York, 1989, pp. 53-61.

[11]Majdalani, J., "Improved Flowfield Models in Rocket Motors and the Stokes Layer with Sidewall Injection," Ph.D. Dissertation, University of Utah, 1995.

[12]Schlichting, H., *Boundary-Layer Theory*, 7th ed., McGraw-Hill Book Company Inc., New York, 1979.

[13]Stokes, G. G., "On the Theories of Internal Friction of Fluids in Motion," *Transactions of the Cambridge Philosophical Society,* Vol. 8, 1845, pp. 287-305.

[14]Richardson, E. G., and Tyler, E., "The Transverse Velocity Gradient near the Mouths of Pipes in Which an Alternating or Continuous Flow of Air is Established," *Proceedings of the Royal Society, London, Series A,* Vol. 42, No. 1, 1929, pp. 1-15.